Journal of Alloys and Compounds, 194 (1993) 303–309
JALCOM 7206

Medium-range structure variations in the solid state amorphizing transformation of metallic alloys by mechanical milling

Kenji Suzuki
Institute for Materials Research, Tohoku University, Katahira 2-1-2, Aoba-ku, Sendai 980 (Japan)

Toshiharu Fukunaga
Department of Crystalline Materials Science, Nagoya University, Furo-cho, Chikusa-ku, Nagoya 464-01 (Japan)

(Received March 13, 1992; in final form May 14, 1992)

Abstract

Based on the measurement of neutron total structure factors, the medium-range structure variations during solid state amorphizing transformation of Ni–V, Ni–Ti, Ni–Zr and Cu–V systems by mechanical milling are examined. The topological mechanism of the crystal-to-amorphous solid state structure transition is demonstrated as the conversion of octahedral structural units into tetrahedral units, the connectivity being modified from vertex-sharing into face- and/or edge-sharing during the mechanical milling process.

1. Introduction

During solid state amorphizing by mechanical milling techniques, atoms in the stable equilibrium crystalline state are mechanically excited, react chemically if necessary, and are frozen into a metastable amorphous solid state with a topologically disordered atomic arrangement. This process is the opposite approach to that of traditional procedures which use quenching from an energized state such as the melt or vapor.

So far several models for the thermodynamic mechanism of crystalline-to-amorphous solid state transformations have been proposed: local melt quenching [1], asymmetric solid state interdiffusion [2], excess defect accumulation [3], lowering of the melting point [4] and phase separation [5] in supersaturated solid solutions, elastic instability [6] and so on. However, the topological evolution of the short-range structure during the transformation by milling from a crystalline to an amorphous solid has been investigated by the neutron total scattering technique [7, 8].

This paper reports on the characterization of the topological and chemical short-range structure, and in particular the evolution of the medium-range structure during mechanical alloying (MA) and mechanical grinding (MG) of Ni–V, Ni–Ti, Ni–Zr and Cu–V binary systems.

2. Experimental details

Both MA and MG processes were carried out at ambient temperature by rotating a stainless steel vial (SUS 304) of 108 mm inner diameter and 105 mm length, which contained about 25 stainless steel balls 14 and 19 mm in diameter, and metallic powder specimens. The rate of rotation of the vial was 80–110 rev min^{-1}. The air in the vial was thoroughly replaced with argon gas to prevent the metallic powders from oxidizing during MA and MG [9].

Spallation pulsed neutrons generated by proton accelerators are useful for characterizing the highly resolved structure of atomic-scale to medium-range length in amorphous alloys, because an incident neutron beam flux is available over a wide range of energy, from epithermal to cold neutrons, and the time-of-flight technique can be properly applied [10]. The neutron total scattering spectrometer HIT, installed at the pulsed neutron source KENS in the National Laboratory for High Energy Physics, Tsukuba was used for measurement of the total structure factors in this work. Detailed procedures for the measurement and data analysis of neutron total scattering have been described in previous work [11, 12].

3. Transition of the structural unit from octahedral to tetrahedral during mechanical alloying and mechanical grinding

The Faber–Ziman [13] neutron total structure factor $S(Q)$ observed for an Ni–V amorphous alloy is written

0925-8388/93/$6.00

as a weighted sum of three partial structure factors $S_{NiNi}(Q)$, $S_{NiV}(Q)$ and $S_{VV}(Q)$:

$$S(Q)=(1/\langle b\rangle^2)[c_{Ni}{}^2b_{Ni}{}^2S_{NiNi}(Q)+2c_{Ni}c_Vb_{Ni}b_VS_{NiV}(Q) + c_V{}^2b_V{}^2S_{VV}(Q)] \quad (1)$$

where c_{Ni} (c_V) and b_{Ni} (b_V) are the concentrations and coherent neutron scattering lengths of nickel (vanadium) nuclei, $\langle b\rangle = c_{Ni}b_{Ni}+c_Vb_V$ and Q is the absolute value of the scattering vector.

The experimental $S(Q)$ value of the Ni–V binary alloy can be approximated only to the Ni–Ni partial structure factor $S_{NiNi}(Q)$ except in the region of extremely low nickel content,

$$S(Q)=S_{NiNi}(Q) \quad (2)$$

because the value of b_V (-0.0382×10^{-12} cm) is negligibly small compared with that of b_{Ni} (1.03×10^{-12} cm). Therefore, we can determine selectively how the nickel (f.c.c.) lattice is modified into an amorphous structure during MA by observing the neutron total structure factor $S(Q)$ as a functional of MA time.

Figure 1 shows changes in the neutron total structure factor $S(Q)$ for the MA of 4Ni(f.c.c.)+6V(b.c.c.)→ Ni_4V_6 (amorphous) [14], where Bragg reflection peaks for the nickel (f.c.c.) crystal are already broadened even before milling by the wide resolution function of the HIT spectrometer used for measurement of liquid and amorphous structure factors. All the Bragg reflection peaks from the nickel (f.c.c.) lattice broaden further with increasing MA time. In particular, a drastic change is seen in the fact that the (200) Bragg reflection peak is practically lost, while the (111) peak is essentially preserved in the final amorphized state. This suggests that octahedral structural units in the nickel (f.c.c.) lattice are totally destroyed during MA and the tetrahedral structural units are well retained in the amorphous structure, as shown in Fig. 2.

The phenomena suggested by $S(Q)$ have been demonstrated in the behavior of the pair correlation function $g(r)$, when the second and fifth peaks are lost dramatically with increasing MA time while the other peaks are only broadened [14]. The second and fifth neighboring atoms in the f.c.c. lattice occupy the key sites in constructing octahedral structural units.

This preferential destruction of octahedral structural units is also observed during amorphization of the NiZr crystalline compound (orthorhombic space group C_{mcm}) by MG [15]. Crystalline NiZr is constructed from both octahedral and tetrahedral structural units as shown in Fig. 3. Two octahedral structural units are connected to each other by a shared face. Two tetrahedral structural units are linked by a shared vertex, edge or face. Octahedral and tetrahedral structural units are connected by the formation of a trigonal prism between the polyhedra. Atomic distances and coordination numbers in Ni–Ni, Ni–Zr and Zr–Zr correlations in crystalline NiZr compound are summarized in Fig. 4. If

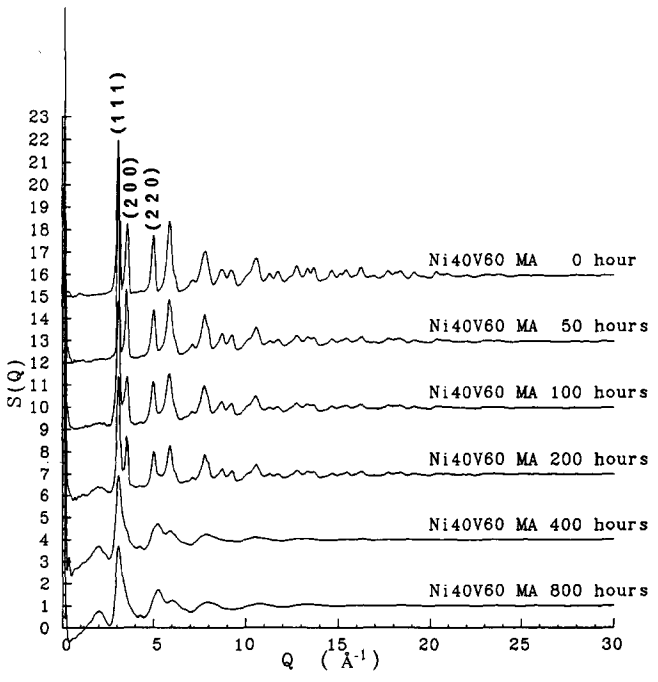

Fig. 1. Neutron total structure factors $S(Q)$ for MA of 4Ni(f.c.c.)+6V(b.c.c.)→Ni_4V_6(amorphous) as a function of milling time.

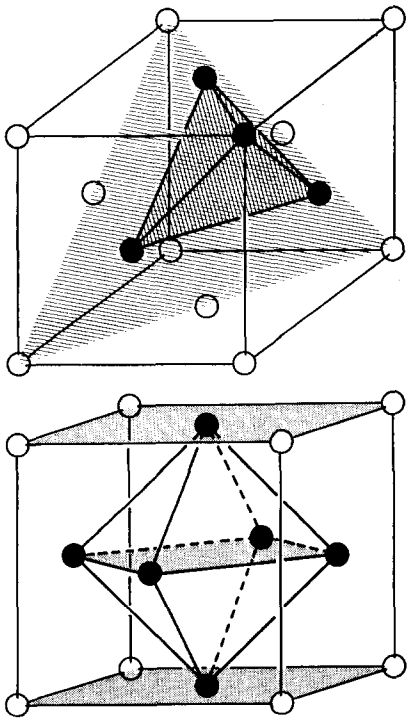

Fig. 2. Tetrahedral and octahedral structural units in an f.c.c. lattice.

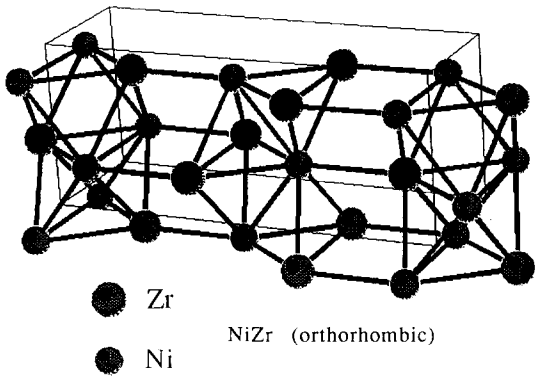

Fig. 3. Atomic arrangement in the NiZr crystalline compound.

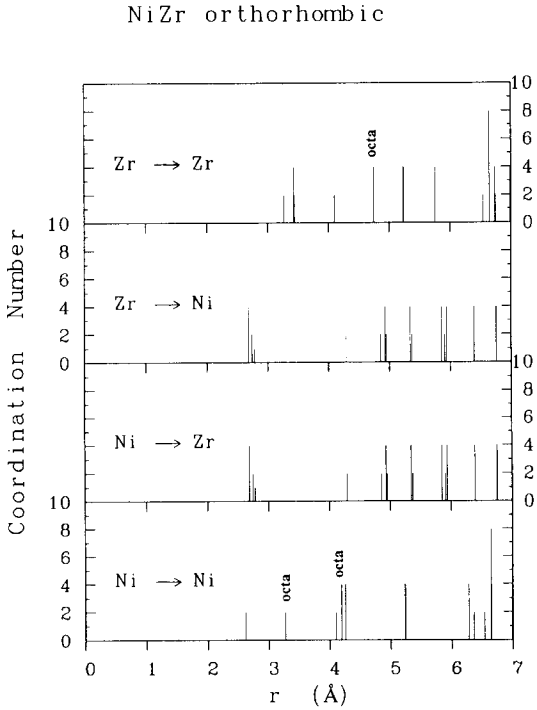

Fig. 4. Atomic distances and coordination numbers of Ni–Ni, Ni–Zr and Zr–Zr correlation in the NiZr crystalline compound.

octahedral structural units are predominantly destroyed in the MG process, we should find a drastic modification of the Ni–Ni correlation located around an atomic distance $r = 4.2$ Å and of the Zr–Zr correlation located around $r = 4.7$ Å, which correspond to the vertex–vertex distances characteristic of an octahedral structural unit.

The phenomenon mentioned above is certainly confirmed in the evolution of $g(r)$ during the MG process for amorphization of crystalline NiZr, as shown in Fig. 5 [7, 15]. The second peak located around $r = 4.2$ Å is lost dramatically and the third peak around $r = 5$ Å is broadened as the MG progresses. It is concluded that the basic mechanism of topological modification from a crystalline to an amorphous solid by MA and MG involves a short-range transition from octahedral

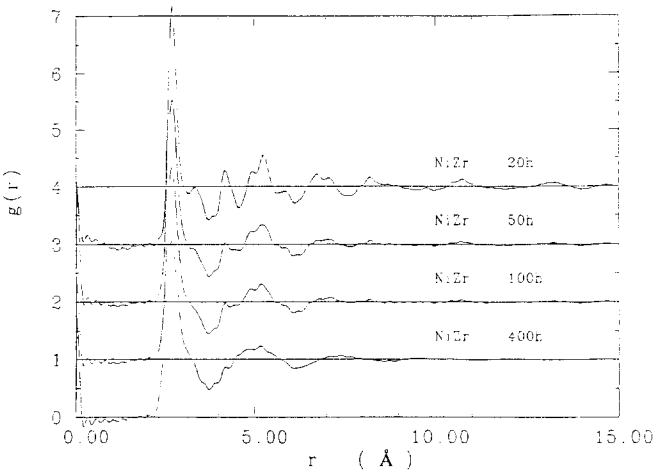

Fig. 5. Neutron total pair distribution functions $g(r)$ of NiZr as a function of milling time.

structural units to the tetrahedral structural units in the solid state.

4. Atomic-scale chemical mixing in mechanically alloyed amorphous alloys

The MA process usually provides a wide range of chemical composition for the formation of amorphous alloys. Ni–V amorphous alloys can be prepared by the MA process in the range 45–70 at.% vanadium, which includes the crystalline σ phase region [16]. However, the overall behavior of neutron total structure factors $S(Q)$, which is almost the same as that of the Ni–Ni partial structure factors $S_{NiNi}(Q)$ is found to be very similar over the whole chemical composition range, as shown in Fig. 6. This means that the Ni–Ni correlation is rigidly preserved without significant change over the whole range of composition of Ni–V amorphous alloys.

Figure 7 shows the coordination numbers of nickel atoms around a nickel atom in Ni–V amorphous alloys obtained from the area under the first peak of the radial distribution functions (RDFs), which are defined as the Fourier transforms of $S(Q)$ truncated of $Q_{max} = 23$ Å^{-1} [16]. The shaded area in Fig. 7 corresponds to the uncertainty contributed by Ni–V and V–V correlations, because we approximate $S(Q) = S_{NiNi}(Q)$ by neglecting $S_{NiV}(Q)$ and $S_{VV}(Q)$. The coordination number for Ni–Ni correlation in Ni–V amorphous alloys is essentially close to that of the crystalline σ phase over a wide range of chemical composition. If nickel and vanadium atoms are assumed to occupy statistically random lattice sites in the σ phase, the coordination number for Ni–Ni correlation does shift toward fairly high values as shown in Fig. 7. This result strongly suggests that the MA process, starting from elemental nickel and vanadium metals, provides atomic-scale mix-

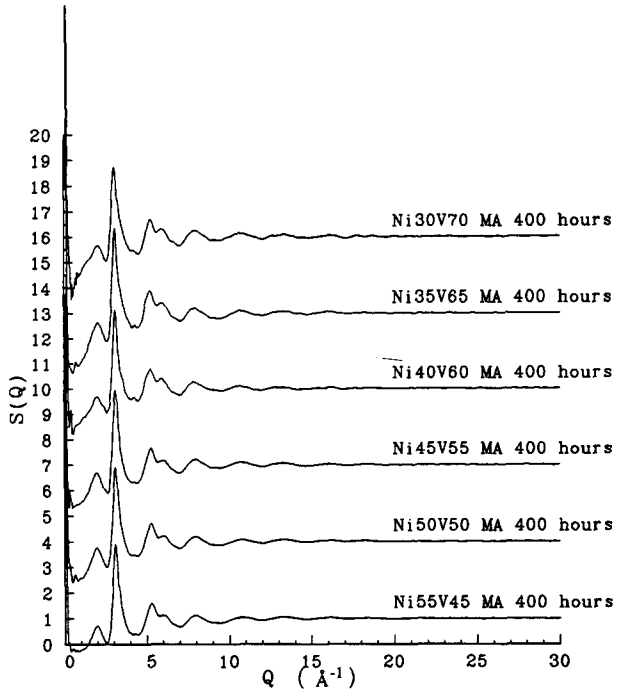

Fig. 6. Neutron total structure factors $S(Q)$ of Ni–V amorphous alloys prepared by MA as a function of vanadium content.

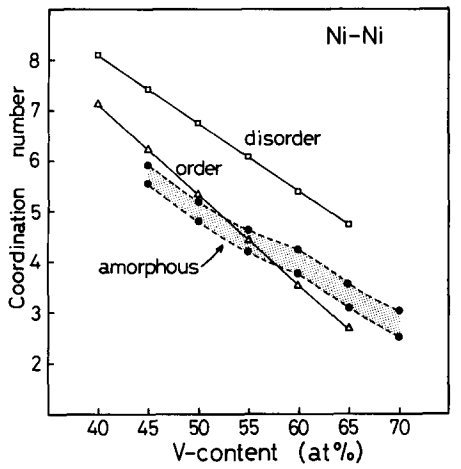

Fig. 7. Coordination numbers of nickel atoms around a nickel atom in MA amorphous alloys, ordered σ phase and disordered σ phase of Ni–V binary system as a function of vanadium content.

ing of metallic elements to form homogeneous Ni–V amorphous alloys in which chemical short-range structures are not a statistically random mixture but are similar to those found in the counterpart crystalline σ phase alloys.

If an amorphous alloy with an average coherent neutron scattering length $\langle b\rangle = 0$ – a so called neutron zero-scattering alloy – is available, the atomic-scale chemical order in the amorphous alloy can be examined directly by observing the Bhatia–Thornton [17] neutron total structure factor $S^{BT}(Q)$:

$$S^{BT}(Q) = (1/\langle b^2\rangle)[\langle b\rangle^2 S_{NN}(Q) + 2\langle b\rangle |\Delta b| S_{NC}(Q) + |\Delta b|^2 S_{CC}(Q)] \quad (3)$$

where $S_{NN}(Q)$ is the partial structure factor associated with density–density correlation, $S_{CC}(Q)$ is the partial structure factor associated with concentration–concentration correlation, and $S_{NC}(Q)$ is the cross term of density–concentration correlation. The Bhatia–Thornton neutron total structure factor $S^{BT}(Q)$ for an $Ni_{24.3}Ti_{75.7}$ neutron-zero scattering alloy only provides the $S_{CC}(Q)$ value associated with the concentration–concentration correlation:

$$S^{BT}(Q) = [|\Delta b|^2/\langle b^2\rangle] S_{CC}(Q) \quad (4)$$

because $b_{Ni} = 1.03\times10^{-12}$ cm, $b_{Ti} = -0.33\times10^{-12}$ cm, $\langle b\rangle = 0$, $\langle b^2\rangle = c_{Ni}b_{Ni}^2 + c_{Ti}b_{Ti}^2 \neq 0$ and $|\Delta b| = |b_{Ni} - b_{Ti}| \neq 0$.

Figure 8 shows how $S^{BT}(Q)$ for a mixture of nickel and titanium crystalline powders is modified into $S_{CC}(Q)$ for an $Ni_{24.3}Ti_{75.7}$ amorphous alloy during MA [18]. The profile of $S_{CC}(Q)$ for the $Ni_{24.3}Ti_{75.7}$ amorphous alloy after an MA time of 800 h is almost the same as that for a melt quenched alloy [19], except in the range $Q < 0.5$ Å^{-1}. We find that an MA time of more than 400 h is needed to obtain the homogeneous structure of atomic-scale alloying.

The reduced radial concentration functions $G(r)$, defined as the Fourier transform of $S^{BT}(Q)$ truncated at $Q_{max} = 30$ Å^{-1}, are shown in Fig. 9 [18]. A very large positive peak appearing around $r = 2.5$ Å, which corresponds to the Ni–Ni nearest-neighbor distance in nickel (f.c.c.) crystal, drastically diminishes, to be modified finally into a negative peak corresponding to the Ni–Ti unlike atom bonding in the $N_{24.3}Ti_{75.7}$ amorphous alloy with increasing MA time. This is direct evidence

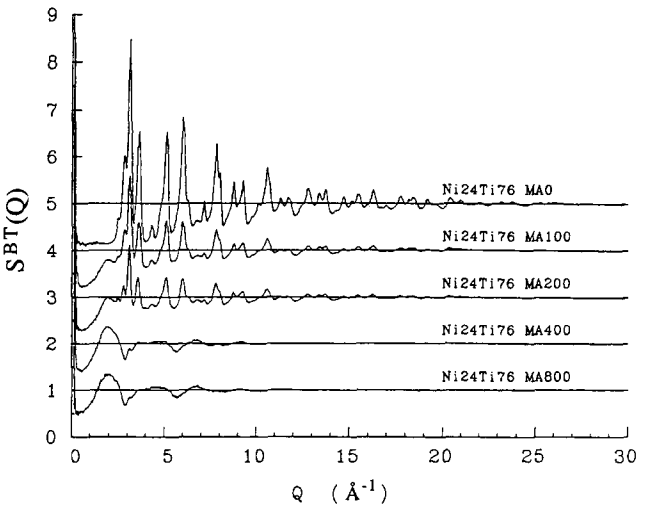

Fig. 8. Bhatia–Thornton total neutron structure factors $S^{BT}(Q)$ for MA of the neutron-zero scattering system 24.3Ni(f.c.c.) + 75.31Ti(hex) → $Ni_{24.3}Ti_{75.3}$ (amorphous) as a function of milling time.

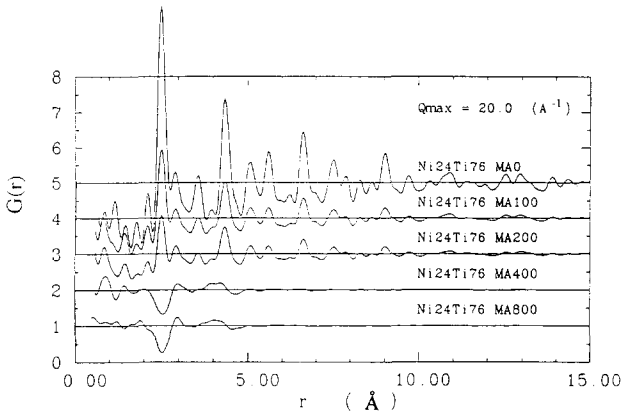

Fig. 9. Bhatia–Thornton total neutron reduced radial concentration functions $G(r)$ for MA of the neutron-zero scattering system 24.3Ni(f.c.c.) + 75.3Ti(h.c.p.) → $Ni_{24.3}Ti_{75.3}$(amorphous) as a function of milling time.

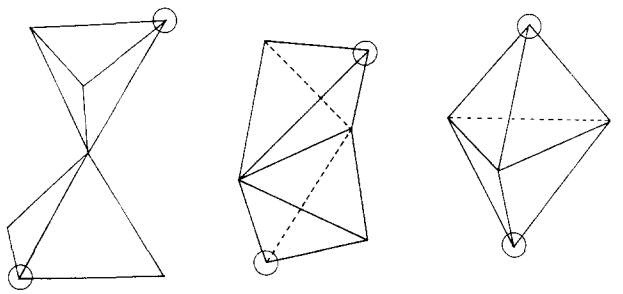

(a) vertex-sharing (b) edge-sharing (c) face-sharing

Fig. 10. Three possible ways of connecting tetrahedral structural units.

for the formation of Ni–Ti chemical bonds at a bond distance of $r = 2.54$ Å in Ni–Ti amorphous alloys by the MA process.

5. Medium-range structure of mechanically alloyed and mechanically ground amorphous alloys

The topological structure of amorphous metals is well approximated by a dense random packing of spherical atoms constructing exclusively tetrahedral structural units [20]. As demonstrated above, octahedral structural units are almost entirely lost during the solid state transition from a crystal line to an amorphous solid by MA and MG processes. Therefore, the medium-range structure of MA and MG amorphous alloys should be characterized by the connectivity between tetrahedral structure units. There are three possible ways of connecting tetrahedra to each other: vertex-sharing, edge-sharing, and face-sharing, as shown in Fig. 10.

As is well known, all atoms in the crystalline σ phase (space group $P4_{2/mnm}$) are distributed among the five topologically different lattice sites, which are defined as centers of the coordination polyhedra consisting of tetrahedra only, as in Frank–Kasper phases [8, 15]. In the five different coordination polyhedra, tetrahedra are connected to each other by vertex-, edge- and face-sharing. An interesting point is to examine how the connectivity between tetrahedral structural units in the crystalline σ phase is modified during the solid state amorphizing transformation by MG.

The Faber–Ziman neutron total structure factors $S(Q)$ are shown as a function of MG time in Fig. 11 [8, 15]. The MG process broadens the Bragg reflection peaks with fewer ripples in the high Q region $Q > 5$ Å^{-1}, and drastically changes the peak profiles located in the low Q region $Q < 4$ Å^{-1}. The first sharp diffraction peak (FSDP), corresponding to the (101) Bragg reflection peak, abruptly diminishes, while the (220) peak barely remains to form a so-called pre-peak, which is often observed in the Ni–Ni partial structure factors of nickel–early transition metal amorphous alloys [21].

Figure 12 shows the neutron total radial distribution functions (RDFs) of Ni_4V_6 alloys defined by Fourier transforming $S(Q)$ truncated at $Q_{max} = 30$ Å^{-1}. The first peak located around $r = 2.5$ Å, corresponding to the Ni–Ni atomic distance in a tetrahedral structural unit, does not change appreciably with increasing MG time. The second peak, appearing around $r = 4$ Å, never shows significant variations in its profile and corresponds very closely to the Ni–Ni distance in intertetrahedral structural units connected by face sharing (Fig. 10(c)). The third peak is located around $r = 5$ Å and is significantly reduced with increasing MG time. The atomic distance $r = 5$ Å corresponds to the Ni–Ni distance in intertetrahedral structural units connected by vertex

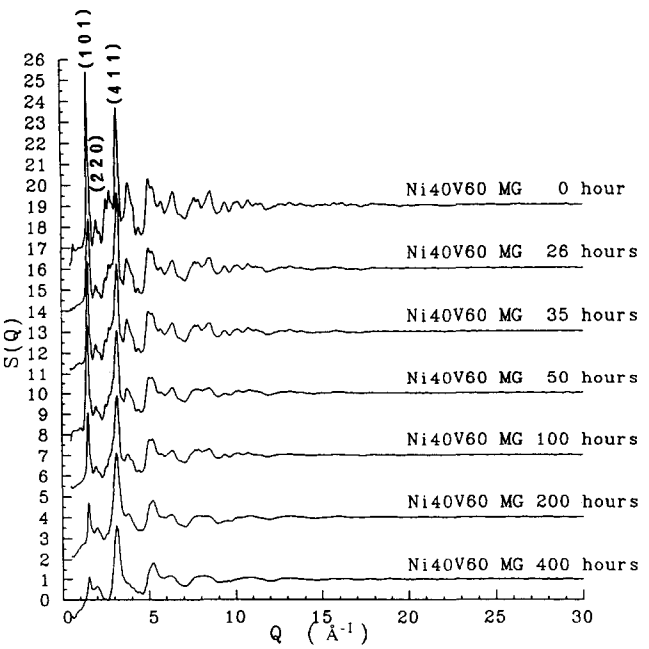

Fig. 11. Neutron total structure factors $S(Q)$ for MG of Ni_4V_6 (crystalline σ phase) → Ni_4V_6 (amorphous) as a function of milling time.

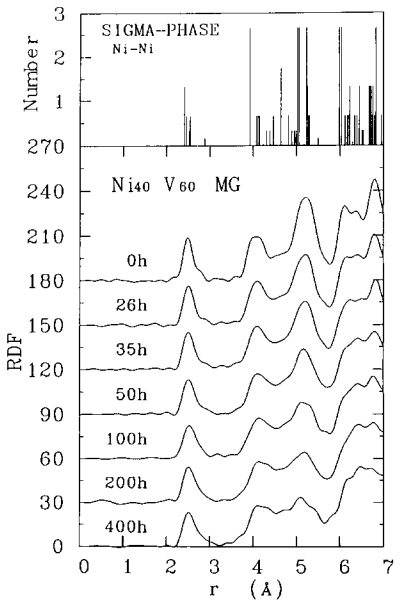

Fig. 12. Neutron total radial distribution functions (RDF) for MG of Ni_4V_6 (crystalline σ phase)→Ni_4V_6(amorphous) as a function of milling time.

sharing (Fig. 10(a)). The Ni–Ni distance of intermediate length $r=4$–5 Å comes partly from edge sharing between tetrahedral structure units.

Based on the characteristic variation in RDF shown in Fig. 12, the formation of medium-range order in Ni_4V_6 amorphous alloys can be understood in terms of the conversion from vertex sharing to face sharing between the tetrahedral structural units of the crystalline σ phase. Vertex sharing between tetrahedral structural units is usually observed in SiO_2 glass and certainly contributes to the FSDP of its $S(Q)$ characteristic [22]. Therefore, a drastic reduction in the (101) Bragg reflection peak of $S(Q)$ of the Ni_4V_6 crystalline σ phase compound demonstrates rapid destruction of vertex sharing between tetrahedral structural units. In contrast, the (220) Bragg reflection peak corresponding to the pre-peak often located around $Q=1.9$ Å^{-1} in $S(Q)$ originates from face sharing between tetrahedral structural units [23]. As face sharing is almost completely preserved in amorphous alloys, the (220) peak does not change with increasing MG time. As shown in Fig. 9, a broad positive peak appearing around $r=4$ in $G(r)$ of the MA $Ni_{24.3}Ti_{75.7}$ amorphous alloy, which corresponds to the second-nearest Ni–Ni distance, also suggests the preferential formation of face sharing between tetrahedral structural units.

6. Nanometer-scale inhomogeneities in mechanically alloyed amorphous alloys

The neutron total structure factor $S(Q)$ of MA amorphous alloys often has significant intensity in the small-angle scattering in the low Q region $Q<0.5$ Å^{-1}, while MG amorphous alloys do not. Figure 13 shows clearly the small-angle scattering intensity of $S(Q)$ of an NiZr MA amorphous alloy [7]. This suggests that MA amorphous alloys still contain nanometer-scale inhomogeneous regions.

In the case of MA processing of Ni–V and Ni–Ti amorphous alloys, as found in Figs. 1 and 8, small-angle scattering intensities appear and saturate rapidly in a relatively early stage of the MA process, before the pre-peak is formed and oscillations in the high Q region are damped in $S(Q)$. This means that small-angle scattering intensities are strongly correlated with the formation of a mixture of nanometer-scale crystalline elemental metal particles, formed by destruction of the long-range order in crystalline elemental metals during an early stage of MA due to the accumulation of crystalline lattice defects such as vacancies, dislocations and so on. In the case of MG of a crystalline compound, nanometer-scale chemical inhomogeneities are not formed and no small-angle scattering appears.

More pronounced small-angle scattering intensities are observed in neutron structure factors $S(Q)$ during MA of Cu–Ta [24] and Cu–V [25] amorphous alloys. Both Cu–Ta and Cu–V systems have positive mixing enthalpies corresponding to an immiscible system in the equilibrium state. As shown in Fig. 14 [25], the overall behavior in the evolution of Bragg reflection peaks in the $S(Q)$ curve of the Cu–V system as a function of MA time is essentially close to that of the Ni–V system which has a negative mixing enthalpy, corresponding to a miscible system in the equilibrium state. This means that the short-range structure characteristic of amorphous alloys is formed in an immiscible system according to nearly the same mechanism as that of a miscible system. However, pronounced small-angle scattering intensities of an immiscible system certainly have their origin in nanometer-scale inhomogeneities owing to the fluctuation in chemical composition as well as topological defects. In fact, the b.c.c. configuration of copper atoms dissolved in a vanadium (b.c.c.)

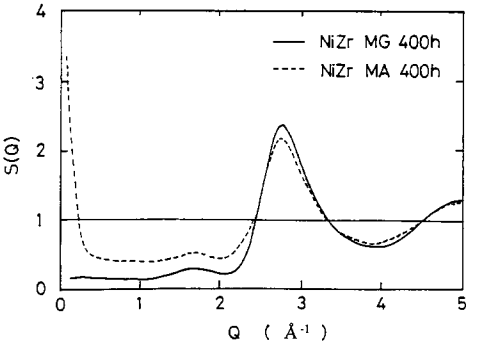

Fig. 13. Small-angle neutron scattering intensities of MA and MG NiZr amorphous alloys.

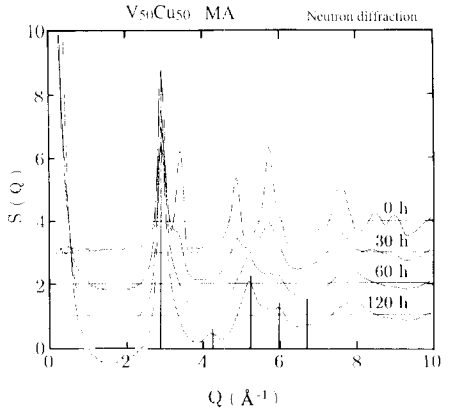

Fig. 14. Neutron total structure factors $S(Q)$ for MA of an immiscible system Cu(f.c.c.) + V(b.c.c.) → CuV(b.c.c. + amorphous) as a function of milling time.

matrix appears in the final stage of MA processing of the Cu–V immiscible system. This MA alloy of the Cu–V system consists of at least two phases, amorphous and b.c.c. solid solutions, which are expected to be dispersed on a nanometer scale.

7. Concluding remarks

The destruction of long-range order in a crystalline lattice by mechanical milling is not directly transferred to the amorphizing transformation in the solid state. Broadening of the Bragg reflection peaks in the crystalline lattice saturates rapidly at an early stage of mechanical milling, and then rearrangements of atoms characteristic of short- and medium-range order occurs during the solid state amorphizing transformation by MA and MG.

The topological mechanism of solid state transformation from a crystalline to an amorphous solid by mechanical milling can be understood in terms of the mutation of octahedral structural units into tetrahedral structural units, and reconnection of tetrahedral structural units from vertex sharing to face and/or edge sharing. However, significant fluctuations persist over a nanometer range in MA amorphous alloys. Even in an immiscible binary system having a positive mixing enthalpy, the appearance of short-range structure characteristic of amorphous alloys and of a more pronounced small-angle scattering intensity are still observed during the evolution of neutron total structure factors.

Careful observations of neutron total scattering over the continuous wide range of $Q = 0.0$ to 50 $Å^{-1}$ should be helpful in investigating the total mechanism of structural evolution in mechanically driven solid state amorphizing transformations. In particular, there is need to focus on the role of low-energy medium-range collective excitation in crystalline-to-amorphous solid state transitions by measurement of neutron dynamical structure factors during MA and MG processing of metallic alloys, which is in progress in our laboratory.

Acknowledgments

The authors would like to express their thanks for support from Grant-in-Aid for Developmental Research (B) 03555139 and for Co-operative Research (A) 03302053 from the Ministry of Education, Science and Culture, Japan.

References

1 A. Y. Yermakov, Y. Y. Yurchikov and V. A. Barinov, *Phys. Met. Metallogr., 52* (1981) 50.
2 R. B. Schwarz, R. R. Petrich and C. K. Saw, *J. Non-Cryst. Solids, 76* (1985) 281.
2 C. C. Koch, O. B. Cavin, C. G. McKamey and J. O. Scarborough, *Appl. Phys. Lett., 43* (1983) 1017.
4 H. J. Fecht, G. Han, Z. Fu and W. L. Johnson, *J. Appl. Phys., 67* (1990) 1744.
5 W. Biegel, W. Schaper, H.-U. Krebs, J. Hoffmann, H. C. Freyhardt, R. Bush and R. Bormann, *Coll. Phys., C4* (1990) C4-189.
6 W. L. Johnson, *Prog. Mater. Sci., 30* (1986) 81.
7 K. Suzuki, *J. Non-Cryst. Solids, 112* (1989) 23.
8 K. Suzuki, *J. Phys. Condens. Matter, 3* (1991) F39.
9 M. S. El-Eskandarany, F. Itoh, K. Aoki and K. Suzuki, *J. Non-Cryst. Solids, 117–118* (1990) 729.
10 K. Suzuki, Glasses. In D. L. Price and K. Sköld (eds.), *Method of Experimental Physics — Neutron Scattering,* Vol. 23B, Academic Press, New York, 1987, Chapter 12, p. 243.
11 K. Suzuki, M. Misawa, K. Kai and N. Watanabe, *Nucl. Instrum. Methods, 147* (1977) 519.
12 K. Suzuki, *J. Non-Cryst. Solids, 117–118* (1990) 1.
13 T. E. Faber and J. M. Ziman, *Philos. Mag., 11* (1965) 153.
14 T. Fukunaga, Y. Homma, M. Misawa and K. Suzuki, *J. Non-Cryst. Solids, 117–118* (1990) 721.
15 Y. Homma, T. Fukunaga, T. Misawa and K. Suzuki, *Mater. Sci. Forum, 88/90* (1992) 339.
16 T. Fukunaga, Y. Homma, M. Misawa and K. Suzuki, *Mater. Sci. Eng., A134* (1991) 987.
17 A. B. Bhatia and D. E. Thornton, *Phys. Rev. B, 2* (1970) 3004.
18 T. Fukunaga, M. Misawa, K. Suzuki and U. Mizutani, *Mater. Sci. Forum, 88/90* (1992) 325.
19 T. Fukunaga, N. Hayashi, N. Kai, N. Watanabe and K. Suzuki, *Physica B, 120* (1983) 352.
20 J. L. Finney and J. Wallace, *J. Non-Cryst. Solids, 43* (1981) 165.
21 T. Fukunaga, S. Urai, N. Watanabe and K. Suzuki, *J. Phys. F, 16* (1988) 99.
22 S. C. Moss and D. L. Price, in D. Adler, H. Fritzsche and S. R. Ovshinsky (eds.), *Physics of Disordered Materials,* Plenum, New York, 1985, p. 77.
23 R. B. Schwarz, personal communication, 1991.
24 T. Fukunaga, K. Nakamura, K. Suzuki and U. Mizutani, *J. Non-Cryst. Solids, 117–118* (1990) 700.
25 T. Fukunaga, M. Mori, K. Inou and U. Mizutani, *Mater. Sci. Eng., A134* (1991) 863.